American Mineralogist, Volume 89, pages 1625–1630, 2004

Quantitative analysis of ammonium in biotite using infrared spectroscopy

VINCENT BUSIGNY,[1,2,*] PIERRE CARTIGNY,[1] PASCAL PHILIPPOT,[2] AND MARC JAVOY[1]

[1]Laboratoire de Géochimie des Isotopes Stables, CNRS-UMR 7047, IPGP et Université Paris VII, 2 place Jussieu, 75252 Paris Cedex 05, France
[2]Laboratoire de Géosciences Marines, CNRS-UMR 7097, IPGP et Universités Paris VI et VII, 2 place Jussieu, 75252 Paris Cedex 05, France

ABSTRACT

The present paper provides a calibration of the Beer-Lambert law allowing the determination of the ammonium (NH_4) content of biotite using infrared (IR) spectroscopy. Single biotite crystals were analyzed by Fourier Transform Infrared spectroscopy. Using a linear correlation between the NH_4 infrared absorption band intensity and the NH_4 content as determined by vacuum techniques, the NH_4 molar absorption coefficient at 1430 cm^{-1} was found to be 441 ± 31 L/mol·cm. After having calibrated the biotite thickness to Si-O absorption band, the NH_4 content of biotite can be calculated directly from its IR spectrum by the relation:

$$[NH_4^+] \text{ (ppm)} = 1044.3 \times \frac{A^{1430} - A^{2395}}{A^{1249} - A^{2395}} - 320$$

where A^{1249}, A^{1430}, and A^{2395} are absorbances corresponding to wavenumbers 1249 cm^{-1} (Si-O vibration peak), 1430 cm^{-1} (NH_4 bending), and 2395 cm^{-1} (spectrum baseline), respectively. The analysis of biotites having different chemical compositions suggests that, to a first approximation, the calibration is independent of biotite chemical composition. An infrared determination of NH_4 partitioning between muscovite and biotite coexisting in the same rocks shows good agreement with results of previous studies and further validates the method.

INTRODUCTION

Nitrogen in crustal rocks occurs mainly as the ammonium ion (NH_4^+). Several infrared studies have shown that ammonium substitutes for potassium in K-bearing minerals due to similar charge and ionic radius (Vedder 1964, 1965; Yamamoto and Nakahira 1966; Karayakin et al. 1973; Higashi 1978). Although analytical techniques are available to measure nitrogen content, in situ quantification of K-bearing minerals remains underused because of a lack of ammonium molecular absorptivity (ε_{NH_4}). In a first contribution, we assessed NH_4 molecular absorptivity in muscovite and presented a method allowing direct NH_4 quantification from IR spectroscopy (Busigny et al. 2003). In the present companion paper, the Beer-Lambert law is calibrated in the case of ammonium ion in biotite. Using a method similar to that of Agrinier and Jendrzejewski (2000) and Busigny et al. (2003), a correlation between biotite thickness and IR absorbance provides an empirical law for thickness spectroscopic measurements. To test the validity of the calibration procedures for both biotite and muscovite, ammonium partitioning between muscovite and biotite coexisting in same rock samples are examined from IR measurements and compared to data available in the literature.

SAMPLES DESCRIPTION

The biotite group, often referred as trioctahedral dark micas, can be described in terms of four end-members: phlogopite–$KMg_3(Si_3AlO_{10})(OH)_2$; annite–$KFe_3(Si_3AlO_{10})(OH)_2$; eastonite–$K(AlMg_2)(Si_2Al_2O_{10})(OH)_2$; and siderophyllite–$K(AlFe_2)(Si_2Al_2O_{10})(OH)_2$. In the present study, several populations of biotite forming solid solutions of these end-members were analyzed, which allows possible effects of chemical composition on the calibration procedure to be tested. Table 1 provides a description of all samples analyzed herein, including the rock types from which biotites were extracted, together with the location of the samples and the mineralogical assemblage of the rock. Biotite grain size ranged approximately between 2 and 15 mm. The mass of biotite grains was between 0.057 and 1.868 mg. Sample thicknesses were restricted from 19 to 215 μm due to handling problem and sensitivity threshold of the IR detector. Micas of 50 to 150 μm thickness produced the best results for IR analyses. To avoid diffraction of the IR light and to allow accurate thickness estimates, IR spectrometry quantification has been performed on samples with homogeneous and parallel faces.

MATERIALS AND METHODS

Infrared measurements were performed on single mica grains using a Fourier Transform Infrared (FTIR) spectrometer (Magna 550, Nicolet) coupled with an optical/IR microscope. Conditions of spectra acquisition include a resolution of 4 cm^{-1}, a mirror velocity of 3.16/cm.s, and a scan number of 300. The IR beam size was approximately 100 μm. All analyses were carried out with an IR beam direction perpendicular to the (001) crystallographic plane (i.e., to the basal layer).

Nitrogen contents were determined using a sealed–tube combustion technique (Boyd et al. 1994; Ader 1999; Busigny et al. 2003). Nitrogen was extracted from single biotite grains during a combustion step, and was purified and separated from other volatiles (mainly H_2O) using CaO (Kendall and Grim 1990). The sealed-tubes were then loaded into a vacuum line and opened with a tube cracker. Combustion gases were transferred using a molecular sieve cooled to liquid nitrogen temperature. Nitrogen was purified and quantified as dinitrogen N_2 by capacitance manometry with an accuracy better than 8% (2σ).

Chemical compositions of biotite were determined using an electron micro-

* E-mail: busigny@ipgp.jussieu.fr

TABLE 1. Rock type from which biotites have been extracted, location of the samples and mineralogical assemblage of the rocks

Sample	Rock type	Location	Lithological context
QGS-35	leucocratic monzonitic granite	Dadaomayang (Qiangtang block, central Tibet)	quartz + perthitic K-feldspar + zoned plagioclase + biotite + accessory zircons
LMMN	leucogranite	Manaslu (Himalaya, central Nepal)	quartz + zoned plagioclase + K-feldspar + microcline + biotite + muscovite + accessory zircons
02-64	kyanite mica-schist	Skjervedalen (Norvege)	quartz + plagioclase + kyanite + garnet + biotite + muscovite + tourmaline + clinochlore + accessory zircons
NO-132	kyanite mica-schist	Rauddalen (Oppland, Norvege)	quartz + plagioclase + kyanite + biotite + apatite + chlorite + staurolite
NS-1	kyanite gneiss	Skjervedalen (Norvege)	quartz + plagioclase + kyanite + biotite + muscovite + rutile + apatite + accessory zircons
NS-3	sillimanite gneiss	Espinouse massif (Montagne Noire, France)	quartz + plagioclase + sillimanite + biotite + muscovite + accessory zircons and apatites
NS-2	andalusite hornstone	Bretagne (France)	quartz + plagioclase + andalusite + biotite + muscovite + graphite + apatite + accessory zircons
99MN04	pegmatite	Caroux massif (Montagne Noire, France)	quartz + perthitic K-feldspar + plagioclase + biotite + muscovite + sillimanite (restite) + accessory zircons
MNPA1	sillimanite migmatite	Dinar (Bretagne, France)	quartz + plagioclase + sillimanite + biotite + muscovite + apatite + accessory zircons

probe (CAMEBAX, University Paris VI). The accelerating voltage was 15 kV and the sample current was 4 nA. The counting times were 40 s for F and 10 s for all other elements. The spot size was 20 μm.

Dark mica infrared spectroscopy and ammonium quantification

The free ammonium ion (NH_4^+) has four normal modes of vibration (Herzberg 1955): a non-degenerate (ν_1), a doubly degenerate (ν_2), and two triply degenerate vibrations (ν_3 and ν_4). All four vibrations are Raman-active, whereas only ν_3 and ν_4 are IR-active. The fundamental frequencies ν_1, ν_2, ν_3, and ν_4, for the free ammonium ion are 3040, 1680, 3145, and 1400 cm^{-1}, respectively (see Harlov et al. 2001, and references therein). A typical absorption spectrum of biotite is shown in Figure 1 for the mid-IR spectral range. Several studies on micas have demonstrated an association between IR absorption bands and mineral chemistry (e.g., Vedder 1964; Karyakin et al. 1973; Farmer 1974; Higashi 1978; Harlov et al. 2001; Beran, 2002). Ammonium absorption bands in biotite correspond to the NH_4-bending vibration "ν_4" at ~1430 cm^{-1} and a series of overlapping bands from 2750 to 3400 cm^{-1}. The overlapping bands arise from the NH_4-stretching vibration "ν_3", combination modes "$\nu_2+\nu_4$", and overtones "$2\nu_2$" and "$2\nu_4$" (Fig. 1). A significant shoulder on the 1430 cm^{-1} band results from a splitting in the degenerate vibrations (Fig. 1). This splitting is likely produced by a reduction of the NH_4^+ tetrahedron symmetry in the mica structure as observed in the case of tobelite (Harlov et al. 2001). The top of the ν_4 absorption band always ranges between 1426 and 1432 cm^{-1}, with no deviation related to biotite chemical composition. An absorption band in the 3580–3630 cm^{-1} region arises from vibrations of hydroxyl groups (Fig. 1). The Si-O stretching vibrations appear in the 800–1200 cm^{-1} region. Combination bands involving the O-H stretching mode and some other lower frequency modes occur in a range from 1730 to 2150 cm^{-1} (Vedder 1964).

The Beer-Lambert law predicts a proportional relationship between ammonium molecular absorbance and concentration in biotite. For a wavenumber of 1430 cm^{-1}, the Beer-Lambert law is of the form:

$$A_{NH_4}^{1430} = d_{biotite} \cdot \varepsilon_{NH_4}^{1430} \cdot [NH_4] \cdot (\rho_{biotite}/M_{NH_4}) \quad (1)$$

where $A_{NH_4}^{1430}$ is the ammonium absorbance (logarithmic unit) at 1430 cm^{-1}, $\rho_{biotite}$ and $d_{biotote}$ are the density (g/cm^3) and the thickness (cm) of the sample, respectively, [NH_4] is the concentration (ppm by weight) of ammonium in biotite, $\varepsilon_{NH_4}^{1430}$ is the molar absorption coefficient (L/mol·cm) of ammonium at 1430 cm^{-1}, and M_{NH_4} is its molecular weight (mg/mol). Assessing the concentration of ammonium by IR spectrometry requires a good knowledge of biotite density and thickness together with ammonium molar absorption coefficient under consideration. Because biotite group densities range between 2.8 and 3.2 g/cm^3 (Nickel and Nichols 1991), we used a constant density value of 3.0 (±0.2) g/cm^3. Sample thickness was measured using a digital micrometer with a precision of ±1 μm. The thickness of a sample is measured after the IR spectrum is obtained and requires the sample to be transferred from the IR spectrometer to a micrometer. This transfer procedure may be a source of inaccuracy if thickness and IR measurements are not performed exactly at the same location.

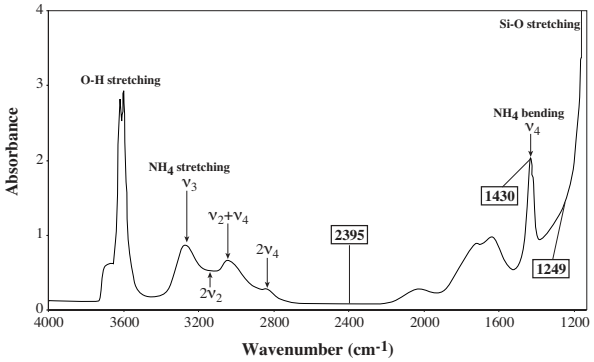

FIGURE 1. Infrared spectrum of a biotite from Skjervedalen mica-schist (sample 02–64). Sample thickness is 173 μm (±10 μm) and ammonium content averages 1204 ppm. See text for a description of the various band assignments.

RESULTS AND DISCUSSION

Chemical composition of biotite samples

Table 2 reports the chemical composition of the different biotites analyzed in this study. Major-element compositions are given in wt% for oxides, and atoms per formula unit (apfu), calculated on the basis of 11 O atoms, also are listed. Table 2 shows that biotite Si-content varies from 2.64 apfu for andalusite hornstone (NS-2) to 2.87 apfu for monzonitic granite (QGS-35). The octaedral Al-content covers a wide range between 0.01 (QGS-35) to 0.67 apfu (LMMN). Magnesium and Fe contents range from 0.33 to 1.70 apfu and 0.80 to 1.55 apfu, respectively. Sample QGS-35 represents a biotite slightly enriched in F (≈0.02 apfu). Such compositional variations may have an influence on IR absorbances used in the present work. Thus, this sample set provides an opportunity to test whether the calibration procedure is applicable to dark micas as a whole, independent of their chemical compositions.

Direct measurement of thickness from silicate network absorption

The potential problem of mechanical measurement of thickness can be overcome by determining the sample thickness

TABLE 2. Biotites chemical composition in major elements

Sample	QGS-35	LMMN	02-64	NO-132	NS-1	NS-3	NS-2	99MN04	MNPA1
SiO_2	37.11	35.80	38.30	35.87	37.11	34.20	33.80	34.95	34.50
TiO_2	3.36	1.88	1.83	1.94	1.33	2.76	2.58	2.84	2.52
Al_2O_3	12.45	19.81	18.07	20.01	19.46	19.65	19.53	20.18	18.74
Cr_2O_3	0.00	0.06	0.15	0.02	0.03	0.00	0.11	0.02	0.08
FeO_T	14.89	22.89	14.54	17.37	12.96	21.25	23.79	20.30	19.67
MnO	0.18	0.65	0.00	0.00	0.01	0.34	0.01	0.22	0.20
MgO	14.77	2.81	13.84	11.55	14.05	6.44	6.10	7.08	8.88
CaO	0.01	0.01	0.01	0.03	0.00	0.00	0.00	0.00	0.00
Na_2O	0.07	0.05	0.24	0.29	0.26	0.12	0.27	0.22	0.15
K_2O	9.61	9.18	8.86	7.92	8.66	9.23	8.64	9.03	9.37
Cl	0.15	0.13	0.10	0.01	0.04	0.00	0.00	0.01	0.01
F	0.71	1.04	0.34	0.22	0.31	0.83	0.00	0.12	0.06
Total	93.32	94.32	96.29	95.24	94.23	94.82	94.84	94.95	94.18
				Formula proportions					
Si	2.872	2.827	2.806	2.681	2.754	2.669	2.639	2.678	2.673
^{IV}Al	1.128	1.173	1.194	1.319	1.246	1.331	1.361	1.322	1.327
^{VI}Al	0.008	0.670	0.366	0.444	0.455	0.476	0.435	0.501	0.384
Cr	0.000	0.004	0.009	0.001	0.002	0.000	0.007	0.001	0.005
Ti	0.195	0.112	0.101	0.109	0.074	0.162	0.152	0.164	0.147
Fe	0.964	1.511	0.891	1.086	0.804	1.387	1.553	1.301	1.274
Mn	0.012	0.043	0.000	0.000	0.001	0.022	0.001	0.014	0.013
Mg	1.704	0.331	1.511	1.287	1.554	0.749	0.710	0.808	1.026
Ca	0.001	0.001	0.001	0.002	0.000	0.000	0.000	0.000	0.000
Na	0.011	0.008	0.034	0.042	0.038	0.019	0.040	0.032	0.023
K	0.949	0.925	0.828	0.755	0.820	0.919	0.861	0.883	0.926
Cl	0.019	0.017	0.013	0.002	0.005	0.000	0.000	0.002	0.002
F	0.174	0.260	0.080	0.053	0.072	0.205	0.000	0.028	0.015

Note: Oxides in wt%, formula proportions calculated on the basis of 11 O atoms.

directly from its IR spectrum. Indeed, for a given mineral, the IR-absorbance of major molecular species is directly proportional to sample thickness (Agrinier and Jendrzejewski 2000; Busigny et al. 2003). In the present work, a relationship between biotite thickness and the silicate network vibration was checked over a large range of wavenumbers, from 1230 to 1340 cm^{-1} and from 2250 to 2650 cm^{-1}. A specific absorbance difference was determined randomly so as to obtain the best possible thickness/absorbance correlation. The best result was obtained for an absorbance difference between 1249 and 2395 cm^{-1} (Fig. 2). The first absorbance at 1249 cm^{-1} is located on high-energy side of the Si-O vibration peak and the second at 2395 cm^{-1} corresponds to the spectrum baseline (Fig. 1), which is related to the measurement conditions (i.e., spectrometer set up, sample surface).

Thickness estimates of biotite ranged from 19 to 215 μm. They are linearly correlated to the absorbance difference between 1249 cm^{-1} and 2395 cm^{-1} (Fig. 2). According to the Beer-Lambert law, absorbance must be zero when thickness is zero, and data can be fitted using the "passing through origin" condition:

$$d_{\text{biotite}}\ (\mu\text{m}) = 130.35 \times (A^{1249} - A^{2395}) \qquad r^2 = 0.984 \qquad (2)$$

where d_{biotite} is the biotite thickness, and A^{1249} and A^{2395} are the absorbance for wavenumbers 1249 and 2395 cm^{-1}, respectively. The precision on thickness measurement using these IR absorbances is better than ±10 μm (2σ; Fig. 2).

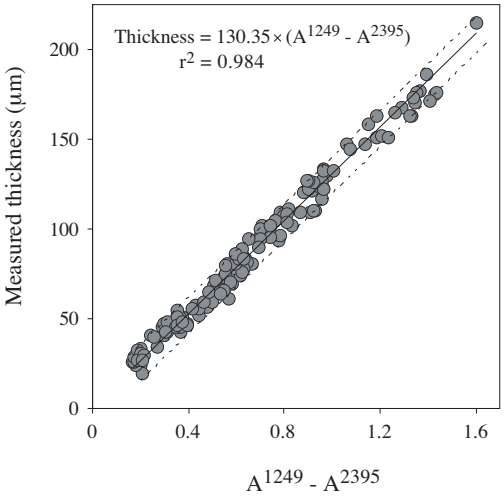

FIGURE 2. Linear relationship observed between sample thickness and difference of IR absorbances ($A^{1249} - A^{2395}$) for biotite. Best-fit line equation allows a determination of biotite thickness directly from its IR spectra. The two dashed lines represent a deviation about the mean line of ±10 μm.

Calibration for the quantification of ammonium in biotite

Because the absorption band at 1430 cm^{-1} corresponds to the superposition of three IR absorbances (see Fig. 1), the position of the baseline associated with ammonium absorbance is difficult to determine. Following the procedure developed for muscovite by Busigny et al. (2003), an absorbance difference between maximum height of the ammonium peak at 1430 cm^{-1} (±5 cm^{-1}) and the spectrum baseline at 2395 cm^{-1} (Fig.1) was preferred rather than the "direct" baseline-corrected ammonium absorbance at 1430 cm^{-1}. The absorbance difference "$A^{1430} - A^{2395}$" corresponds to the sum of the NH_4 bending absorption band ($A^{1430}_{N\text{-}H}$) and the absorbance of the superimposed network vibration (A_{network}). The Beer-Lambert law (Eqn. 1) can be written as:

$$\left[NH_4\right] = \frac{M_{NH_4}}{\rho_{\text{biotite}} \cdot \varepsilon^{1430}_{NH_4}} \times \frac{A^{1430}_{NH_4}}{d_{\text{biotite}}} \qquad (3)$$

where $[NH_4]$, M_{NH4}, $\rho_{biotite}$, $\varepsilon^{1430}_{NH_4}$, and $A^{1430}_{NH_4}$ are defined as in Equation 1. The absorbance of the silicate network is a direct function of the thickness, thus $(A_{network} - A^{2395}) = b \cdot d_{biotite}$ where b is a constant. Because $A^{1430}_{NH_4} = A^{1430} - A_{network}$, the NH_4 bending absorption band can be expressed as:

$$A^{1430}_{NH_4} = A^{1430} - (A^{2395} + b \cdot d_{biotite}) \quad (4)$$

Using Equations 3 and 4, the ammonium content in biotite can be written as:

$$[NH_4^+] = \frac{M_{NH_4}}{\rho_{biotite} \cdot \varepsilon^{1430}_{N\text{-}H}} \times \frac{\left(A^{1430} - A^{2395}\right)}{d_{biotite}} - \frac{M_{NH_4} \cdot b}{\rho_{biotite} \cdot \varepsilon^{1430}_{N\text{-}H}} \quad (5)$$

Equation 5 predicts a linear relationship between ammonium content and [ammonium absorbance/biotite thickness] ratio [i.e., $(A^{1430} - A^{2395})/d_{biotite}$].

Nitrogen contents were measured on 26 single biotite grains, previously analyzed by FTIR spectrometry. Table 3 reports sample weight, sample thickness calculated using Equation 2, the ammonium absorbance/thickness ratio, and ammonium content determined by the sealed-tube extraction technique. Ammonium contents of biotite range between 93 and 2445 ppm NH_4. Figure 3 plots ammonium content vs. ammonium absorbance/thickness ratio. Each point corresponds to a single biotite grain. To avoid possible effects of grain inhomogeneity, ammonium absorbance/thickness ratios were determined from the mean value of several IR analyses ($n > 4$) performed at different locations on the same grain. Figure 3 shows that ammonium content varies linearly with ammonium absorbance/thickness ratio. The relationship is of the form:

$$[NH_4^+] \text{ (ppm)} = 13.6 \times \frac{A^{1430} - A^{2395}}{d_{biotite} \text{ (cm)}} - 320 \quad (6)$$

where $[NH_4^+]$ is a function of thickness and two IR absorbances (A^{1430} at 1430 cm^{-1} and A^{2395} at 2395 cm^{-1}). We emphasize here that the correlation does not intersect the origin of the plot as a consequence of the use of an absorbance difference rather than a "direct" baseline-corrected absorbance. From the Equations 2 and 6, ammonium concentration can be expressed as:

$$[NH_4^+] \text{ (ppm)} = 1044.3 \times \frac{A^{1430} - A^{2395}}{A^{1249} - A^{2395}} - 320 \quad (7)$$

where A^{1249} is the IR absorbance at 1249 cm^{-1}. Equation 7 permits the determination of ammonium concentration in biotite directly by IR spectrometry with a precision better than 20% (2σ) for biotite crystals thicker than 30 μm. For thickness less than 30 μm, the precision dramatically drops (<50%) as a result of the small differences between sample and background IR intensities.

As the values for M_{NH4} and $\rho_{biotite}$ are known, the slope of the linear correlation determined in Figure 3 allows an assessment of the ammonium molar absorption coefficient $\varepsilon^{1430}_{NH_4}$ at 441 ± 31 l/mol cm. The error on $\varepsilon^{1430}_{NH_4}$ is essentially due to the error on $\rho_{biotite}$, which was considered constant at 3.0 (±0.2) g/cm^3. The good linear regression obtained in Figure 3 implies that $\varepsilon^{1430}_{NH_4}$ in biotite is independent of NH_4 content. It is worth noting that $\varepsilon^{1430}_{NH_4}$ estimate for biotite is almost identical to that previously assessed for muscovite (462 ± 32 L/mol·cm) by Busigny et al. (2003).

TABLE 3. Sample weight, calculated thickness, ammonium absorbance/thickness ratio and ammonium content of single biotite crystals

Sample	Weight (mg)	Calculated thickness (μm)	$A^{1430} - A^{2395}$/thickness (cm^{-1})	$[NH_4^+]$ (ppm)
QGS-35-1	0.100	39	30	112 (±57)
QGS-35-3	0.088	45	31	93 (±27)
LMMN-1	0.172	47	69	687 (±83)
LMMN-2	0.118	37	70	779 (±103)
LMMN-3	0.276	95	72	677 (±72)
02-64-1	1.033	173	113	1163 (±98)
02-64-2	0.114	31	126	1653 (±174)
02-64-3	0.399	75	114	1103 (±100)
NO-132-1	0.293	84	84	808 (±81)
NO-132-2	0.519	89	98	1197 (±105)
NO-132-3	0.168	56	93	990 (±108)
NS-1-1	0.577	97	158	1865 (±158)
NS-1-2	1.099	138	156	1823 (±150)
NS-1-3	0.522	95	152	1942 (±165)
NS-3-1	0.338	140	54	301 (±38)
NS-3-2	0.321	117	53	342 (±42)
NS-3-3	0.136	79	54	398 (±67)
NS-2-1	0.153	86	190	2268 (±213)
NS-2-2	0.057	59	204	2445 (±280)
NS-2-3	0.147	56	198	2145 (±204)
99MN04-1	0.401	54	69	597 (±60)
99MN04-2	1.868	74	69	548 (±47)
MNPA1-1	0.095	45	91	850 (±119)
MNPA1-2	0.901	136	96	919 (±79)
MNPA1-3	1.198	110	90	790 (±67)
MNPA1-4	0.188	113	89	910 (±98)

Notes: Sample thickness was calculated from IR spectra using Equation 2 with a precision of ±10 μm. Ammonium content was determined by a sealed-tube extraction technique, with an uncertainty (value in parenthesis) depending mainly on the total amount of extracted nitrogen.

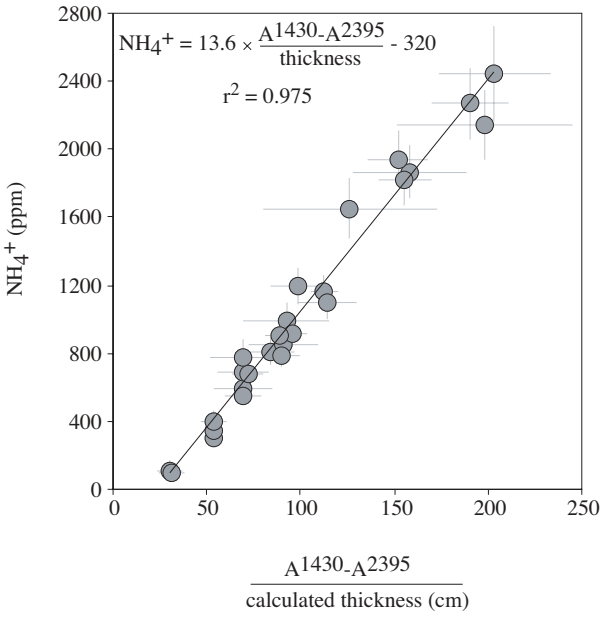

FIGURE 3. Linear correlation between ammonium concentration (ppm) and ammonium absorbance/sample thickness ratio (cm^{-1}). From the line slope, ammonium molecular absorptivity coefficient at 1430 cm^{-1} can be estimated at 441 ± 31 L/mol·cm.

Figures 2 and 3 show that biotites display very good correlations between crystal thickness vs. absorbance and NH_4 content vs. ammonium absorbance/thickness ratio, respectively. These correlations indicate that the influence of chemical composition over the range of investigated samples (Table 2) is negligible. Accordingly, IR calibration procedures for determination of thickness (Eq. 2) and NH_4 content (Eq. 5) seem to be independent of biotite chemical compositions.

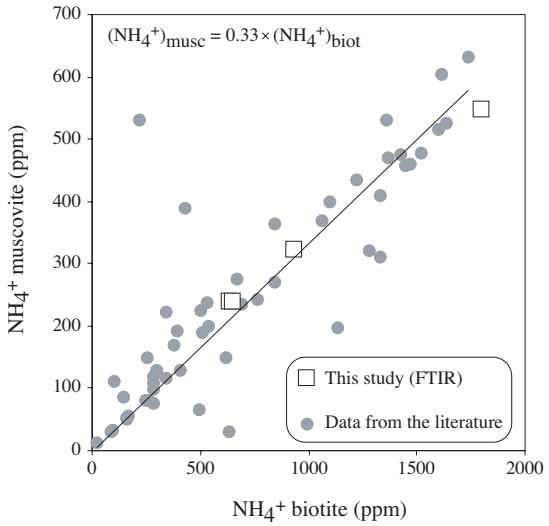

FIGURE 4. Ammonium content of muscovite and biotite coexisting in the same rock samples. Data of this study were calculated from FTIR analyses. Data from the literature correspond to values determined by different chemical extraction methods (Honma and Itihara 1981; Duit et al. 1986; Boyd 1997; Boyd and Philippot 1998; Sadofsky and Bebout 2000).

TABLE 4. Ammonium concentration (calculated from FTIR data) and partitioning coefficient ($K^{[NH_4+]}_{musco-biot}$) of muscovites and biotites coexisting in the same rocks

Sample	$[NH_4^+]_{muscovite}$ (ppm)	$[NH_4^+]_{biotite}$ (ppm)	$K^{[NH_4+]}_{musco-biot}$
LMMN	230	632	
	233	637	
	256	668	
Average	240	646	0.37
NS-1	647	1835	
	476	1798	
	522	1748	
Average	548	1793	0.31
99MN04	217	630	
	244	632	
	244	–	
	257	–	
Average	241	631	0.38
MNPA-1	330	922	
	257	985	
	383	913	
	–	899	
Average	323	930	0.35

Notes: For each rock sample, several mica grains were analyzed in order to provide an average value of NH_4 content. Partitioning coefficient is calculated from this average value.

Ammonium partitioning between biotite and muscovite

Since the early 1980s, the partitioning behavior of NH_4 between muscovite and biotite has been well-documented (Honma and Itihara 1981; Duit et al. 1986; Boyd 1997; Boyd and Philippot 1998; Sadofsky and Bebout 2000). Ammonium has been shown to partition strongly into biotite compared to muscovite (e.g., Honma and Itihara 1981; Duit et al. 1986), a result explained by the larger size of the biotite interlayer site (Honma and Itihara 1981). Figure 4 reports NH_4 concentrations in muscovite vs. biotite for data available in the literature (see caption). Although a slight scattering likely arises from some disequilibrium chemical systems, the data display a good correlation as a result of almost constant partitioning between biotite and muscovite. Using the whole data reported in Figure 4, the partitioning coefficient ($K^{[NH^{4+}]}_{musco-biot}$) is found to average 0.33, which is in good agreement with previous assessments (0.43–Honma and Itihara 1981; 0.33–Duit et al. 1986; 0.32–Boyd 1997). The relative constancy of $K^{[NH^{4+}]}_{musco-biot}$ can be used to check the validity of NH_4 quantification in micas by infrared spectroscopy.

NH_4 content of biotite and muscovite coexisting in the same rocks (99MN04, LMMN, MNPA-1 and NS-1) were estimated from FTIR analyses and are reported in Table 4. These concentrations range from 630 to 1835 ppm and from 217 to 647 ppm in biotites and muscovites, respectively. Values of $K^{[NH^{4+}]}_{musco-biot}$ estimated from average NH_4 contents range from 0.31 to 0.38 (Table 4), which compares well with the average value calculated from data of the literature (i.e., 0.33). This result is illustrated by the Figure 4, in which micas analyzed by IR spectrometry (this study) are situated on the same correlation that micas measured by other workers using independent chemical methods. This observation strongly supports the validity of IR quantification procedures for dark and white micas.

ACKNOWLEDGMENTS

Harald Behrens, Ray Frost, and an anonymous reviewer are greatly thanked for their constructive comments. Philippe Agard, Françoise Roger, and Nicole Santarelli are gratefully acknowledged for providing rock samples. Michel Girard, Jean-Jacques Bourrand, and Karine Leblanc are thanked for their technical assistance. Marc Quintin is thanked for making thin sections. Contribution IPGP 1971 and CNRS 361.

REFERENCES CITED

Ader, M. (1999) Histoire isotopique de l'azote organique de la diagénèse au métamorphisme. Ph.D. thesis, Université Paris 7, IPGP, France, p. 144–181.

Agrinier, P. and Jendrzejewski, N. (2000) Overcoming problems of density and thickness measurements in FTIR volatile determinations: a spectroscopic approach. Contribution to Mineralogy and Petrology, 139, 265–272.

Beran, A. (2002) Infrared spectroscopy of micas. In A. Mottana, F.P. Sassi, J.B. Thompson, S. Guggenheim, Ed., Micas: crystal chemistry and metamorphic petrology, p. 351–369. Reviews in Mineralogy and Geochemistry, Mineralogical Society of America, Washington, D.C.

Boyd, S.R. (1997) Determination of the ammonium content of potassic rocks and minerals by capacitance manometry: a prelude to the calibration of FTIR microscopes. Chemical Geology, 137, 57–66.

Boyd, S.R. and Philippot, P. (1998) Precambrian ammonium biogeochemistry: a study of the Moine metasediments, Scotland. Chemical Geology, 144, 257–268.

Boyd, S.R., Rejou-Michel, A., and Javoy, M. (1994) Noncryogenic purification of nanomole quantities of nitrogen gas for isotopic analysis. Analytical Chemistry, 66, 1396–1402.

Busigny, V., Cartigny, P., Philippot, P., and Javoy, M. (2003) Ammonium quantification in muscovite by infrared spectroscopy. Chemical Geology, 198, 21– 31.

Duit, W., Jansen, J.B.H., Van Breemen, A., and Bos, A. (1986) Ammonium micas in metamorphic rocks as exemplified by dome de l'Agout (France). American Journal of Science, 286, 702–731.

Farmer, V.C. (1974) The layer silicates. In V.C. Farmer, Ed., The infrared spectra

of minerals, p. 331–363. Mineralogical Society, London.
Harlov, D.E., Andrut, M., and Pöter, B. (2001) Characterisation of tobelite $(NH_4)Al_2(AlSi_3O_{10})(OH)_2$ and ND_4-tobelite $(ND_4)Al_2(AlSi_3O_{10})(OD)_2$ using IR spectroscopy and Rietveld refinement of XRD spectra. Physics and Chemistry of Minerals, 28, 268–276.
Herzberg, G. (1955) Infrared and Raman spectra of polyatomic molecules. Van Nostrand, New York.
Higashi, S. (1978) Dioctaedral mica minerals with ammonium ions. Mineralogical Journal, 9, 16–27.
Honma, H. and Itihara, Y. (1981) Distribution of ammonium in minerals in metamorphic and granitic rocks. Geochimica et Cosmochimica Acta, 45, 983–988.
Karyakin, A.V., Volynets, V.F., and Krieventsova, G.A. (1973) Investigation of nitrogen compounds in micas by infrared spectroscopy. Geochemistry International, 3, 326–329.
Kendall, C. and Grim, E. (1990) Combustion tube method for measurement of nitrogen isotope ratios using calcium oxide for total removal of carbon dioxide and water. Analytical Chemistry, 62, 525–529.
Nickel, E.H. and Nichols, M.C. (1991) Mineral Reference Manual. p. 8, 23, 164 and 192. Van Nostrand Reinhold, New York.
Sadofsky, S.J. and Bebout, G.E. (2000) Ammonium partitioning and nitrogen-isotope fractionation among coexisting micas during high temperature fluid-rock interactions: examples from the New England Appalachians. Geochimica et Cosmochimica Acta, 64, 2835–2849.
Vedder, W. (1964) Correlations between infrared spectrum and chemical composition of mica. American Mineralogist, 49, 736–768.
———(1965) Ammonium in muscovite. Geochimica et Cosmochimica Acta, 29, 221–228.
Yamamoto, T. and Nakahira, M. (1966) Ammonium in sericites. American Mineralogist, 51, 1775–1787.

MANUSCRIPT RECEIVED AUGUST 8, 2003
MANUSCRIPT ACCEPTED MAY 30, 2004
MANUSCRIPT HANDLED BY GRAY BEBOUT